

RESEARCH ON EIGEN-MODE OF COAXIAL OUTER CORRUGATED RESONATOR

Shenyong Hou^{1, 2, *}, Sheng Yu¹, and Hongfu Li¹

¹Terahertz Science and Technology Research Center, University of Electronic Science and Technology of China, Chengdu 610054, China

²Yangtze Normal University, Chongqing 408001, China

Abstract—For the coaxial outer corrugated resonator, dispersion equations of TE and TM modes are derived by the surface impedance theory, and the first order transmission line equations with mode coupling coefficients are deduced by means of the transmission line and coupling wave theory. According to them, resonant frequency, diffractive quality factor and field profile of geometry of the eigen-mode about the coaxial outer corrugated resonator can be calculated. The effect of outer slot depth, tooth width as well as asymptotic angle of outer conductor and slope angle of inner conductor on resonant frequency and quality factor can be researched. Results show that changes of the outer slot depth and tooth width slightly affect the field frequency and quality factor and that the changes of the asymptotic angle of outer conductor and slope angle of inner conductor almost do not affect field frequency, but greatly affect quality factor.

1. INTRODUCTION

Coaxial corrugated resonator is a kind of important microwave device in high-power, high-frequency gyrotron. Since they have many advantages of rarefying mode spectrum [1, 2], suppressing mode competition [3, 4], reducing microwave ohmic losses [5–7], improving efficient of beam-wave interaction [8, 9] in gyrotrons, they have been applied in controlled fusion experiment [10–13] and suppression of plasma instabilities [14–16]. In the process of the research on gyrotrons, the calculation of eigen-mode has always been an important work. For cylindrical resonators, the eigen-mode in view of the mode coupling of different fields has been studied in detail [17]. For coaxial inner

Received 5 December 2012, Accepted 29 March 2013, Scheduled 25 April 2013

* Corresponding author: Shenyong Hou (houshenyong@sohu.com).

corrugated resonators, some researches on the eigen-mode have been carried out [18]. But, researches on the eigen-mode of the coaxial outer corrugated resonator have seldom been found. The main reason is that it is difficult to derive the mode coupling coefficients because the structure of the coaxial outer corrugated resonator is more complicated. On the other hand, the calculation of eigen-mode becomes complex by second order transmission line equations with mode coupling coefficients. To overcome these difficulties, the paper uses surface impendent theory to get eigen-equations of TE and TM modes and applies transmission and coupling wave theory to obtain the first order transmission line equations with mode coupling coefficients.

The paper is organized as follows: In Section 2, dispersion equations of TE and TM modes are derived from surface impedance theory. In Section 3, the first-order transmission line equation with mode coupling coefficients is established by the transmission line theory. In Section 4, mode coupling coefficients are derived by the coupling wave theory. In Section 5, the resonant frequency, quality factor and field profiles geometry of the eigen-mode of coaxial outer corrugated resonators are calculated. Section 6 is the summary.

2. DISPERSION EQUATION

The coaxial outer corrugated resonator is shown in Fig. 1. Fig. 1(a) shows cross section region, Fig. 1(b) shows unfolded scheme of corrugated region, where $R_i(R_o)$ denotes the inner(outer) radius, d the depth of outer corrugation, l the outer tooth width, s the period of outer corrugation, N the numbers of outer slot, and ϕ_s the azimuthal angle of each slot. There are two methods obtaining dispersion

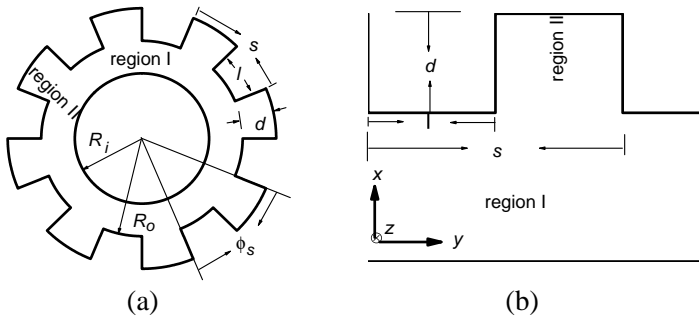


Figure 1. (a) Cross section. (b) Unfolded scheme of outer corrugated region.

equation: one is field matching method(RFM), and the other is surface impedance method(SIM) [4]. Though RFM deals with high field problem, the dispersion equation derived by it is complex, which is not convenient for numerical calculation. However, if a sufficiently large number of slots on outer coaxial conductor, i.e., $s < \frac{\pi R_i}{m}$, where $s = \frac{2\pi R_o}{N}$, simple dispersion equation can be derived by SIM.

For TM_{mn} , under given condition, the surfaces $r = R_i$ and $r = R_o$ behave as boundaries of perfect conduction [4]. Therefore, the dispersion equation of the coaxial outer corrugated resonator is the same as smooth-wall coaxial resonator [18]

$$J_m(\nu_{mn})Y_m\left(\frac{\nu_{mn}}{C}\right) - J_m\left(\frac{\nu_{mn}}{C}\right)Y_m(\nu_{mn}) = 0. \quad (1)$$

For TE_{mn} , fields in the region I may express

$$\begin{cases} \mathbf{E}_r^I = j\frac{m}{r}Z_{mn}(k_{mn\perp}r)V_{mn}(z)\exp(-jm\varphi), \\ \mathbf{E}_\varphi^I = k_{mn\perp}Z'_{mn}(k_{mn\perp}r)V_{mn}(z)\exp(-jm\varphi), \\ \mathbf{H}_z^I = -j\frac{k_{mn\perp}^2}{kZ_0}Z_{mn}(k_{mn\perp}r)V_{mn}(z)\exp(-jm\varphi), \end{cases} \quad (2)$$

where the cylindrical function $Z_{mn}(k_{mn\perp}r) = A_{mn}J_m(k_{mn\perp}r) + B_{mn}Y_m(k_{mn\perp}r)$. Fields in the region II can be expressed by a part of a rectangular TE_{01} mode with field components

$$\begin{cases} \mathbf{E}_y^{II} = -k_{mn\perp}D_{10}V_{mn}(z)\sin(k_\perp x), \\ \mathbf{H}_z^{II} = -j\frac{k_{mn\perp}^2}{kZ_0}D_{10}V_{mn}(z)\cos(k_\perp x). \end{cases} \quad (3)$$

According to SIM, the dispersion equation of the coaxial outer corrugated resonator is

$$\frac{J'_m(\chi_{mn}/C)}{Y'_m(\chi_{mn}/C)} = \frac{wJ_m(\chi_{mn}) + J'_m(\chi_{mn})}{wY_m(\chi_{mn}) + Y'_m(\chi_{mn})}, \quad (4)$$

where $C = \frac{R_o}{R_i}$, $w = \frac{s-l}{s} \tan(\frac{\chi_{mn}d}{R_o})$ is the normalized surface impedance of outer corrugated region. $J_m(\chi)$ and $Y_m(\chi)$ are the Bessel and Neumann functions, with derivatives referring to their argument, and m is the number of field cyclic variations with ϕ (azimuthal index). $k_{mn\perp} = \frac{\chi_{mn}}{R_o}$ is transverse wave number, $k = \frac{\omega}{c}$ and $Z_0 = \sqrt{\frac{\mu_0}{\varepsilon_0}}$ are wave number and wave impedance of free space, respectively.

When $w = 0$, i.e., $d = 0$, (4) becomes dispersion equation of coaxial resonator

$$\frac{J'_m(\chi_{mn}/C)}{Y'_m(\chi_{mn}/C)} = \frac{J'_m(\chi_{mn})}{Y'_m(\chi_{mn})}. \quad (5)$$

Since mode wave functions keep relation [18]

$$\begin{cases} \mathbf{e}_{mn}^{(1)} = -\nabla_t \Phi_{mn}^{(1)}, \\ \mathbf{e}_{mn}^{(2)} = \mathbf{i}_z \times \nabla_t \Phi_{mn}^{(2)}, \end{cases} \quad (6)$$

they satisfy

$$\begin{cases} \nabla_t^2 \Phi_{mn}^{(i)} + \left(k_{mn}^{(i)}\right)^2 \Phi_{mn}^{(i)} = 0, \\ \Phi_{mn}^{(1)}|_c = 0, \frac{\partial \Phi_{mn}^{(2)}}{\partial n}|_c = 0, \end{cases} \quad (7)$$

where c is the wall surface of the coaxial outer corrugated resonator and n the normal to the wall surface.

According to Equations (1), (4), (6) and (7), membrane function $\Phi_{mn}^{(1)}$ and $\Phi_{mn}^{(2)}$ can read

$$\begin{aligned} \Phi_{mn}^{(1)} = & \sqrt{\frac{\pi}{2\varepsilon_m}} \frac{1}{G_{mn}} \left\{ Y_m\left(\frac{\nu_{mn}}{C}\right) J_m\left(\frac{\nu_{mn}}{R_o}r\right) \right. \\ & \left. - J_m\left(\frac{\nu_{mn}}{C}\right) Y_m\left(\frac{\nu_{mn}}{R_o}r\right) \right\} \cos(m\varphi), \end{aligned} \quad (8)$$

$$\begin{aligned} \Phi_{mn}^{(2)} = & \sqrt{\frac{\pi}{2\varepsilon_m}} \frac{1}{K_{mn}} \left\{ Y'_m\left(\frac{\chi_{mn}}{C}\right) J_m\left(\frac{\chi_{mn}}{R_o}r\right) \right. \\ & \left. - J'_m\left(\frac{\chi_{mn}}{C}\right) Y_m\left(\frac{\chi_{mn}}{R_o}r\right) \right\} \cos(m\varphi), \end{aligned} \quad (9)$$

where

$$\varepsilon_m = \begin{cases} 2, & (m = 0) \\ 1, & (m \neq 0) \end{cases} \quad (10)$$

$$G_{mn} = \left\{ \frac{J_m^2\left(\frac{\nu_{mn}}{C}\right)}{J_m^2(\nu_{mn})} - 1 \right\}^{1/2}, \quad (11)$$

$$\begin{aligned} K_{mn} = & \left\{ \left(1 + w^2 - \left(\frac{m}{\chi_{mn}} \right)^2 \right) \left[\frac{Y'_m\left(\frac{\chi_{mn}}{C}\right)}{wY_m(\chi_{mn}) + Y'_m(\chi_{mn})} \right]^2 \right. \\ & \left. - \left(1 - \left(\frac{mC}{\chi_{mn}} \right)^2 \right) \right\}^{1/2}, \end{aligned} \quad (12)$$

where ν_{mn} and χ_{mn} are determined by (1) and (4), respectively.

By applying the continuity condition of z -component of the magnetic field H_z at $r = R_o$, the membrane function of TE₀₁ in the outer corrugation region can be expressed

$$\Phi_o = \sqrt{\frac{\pi}{2\varepsilon_m}} \frac{Y'(\chi_{mn}/C)J_m(\chi_{mn}) - J'(\chi_{mn}/C)Y_m(\chi_{mn})}{K_{mn}} \frac{\cos(m\phi_s)}{\cos(\chi_{mn}d/R_o)} \cos\left(\frac{\chi_{mn}}{R_o}x\right) \quad (13)$$

where ϕ_s is the azimuthal angle of each slot in Fig. 1(a).

3. TRANSMISSION LINE EQUATIONS

The transmission line equations with free source are the basis for researching high field properties. The different structures of a resonator have different formats of transmission line equations. According to Maxwell's equations with free source

$$\begin{cases} \nabla \times \mathbf{E} = -j\omega\mu\mathbf{H}, \\ \nabla \times \mathbf{H} = j\omega\varepsilon\mathbf{E}, \\ \nabla \cdot (\varepsilon\mathbf{E}) = 0, \\ \nabla \cdot (\mu\mathbf{H}) = 0, \end{cases} \quad (14)$$

where $\mathbf{E} = \mathbf{E}_t + \mathbf{E}_z$, $\mathbf{H} = \mathbf{H}_t + \mathbf{H}_z$. $\mathbf{E}_t(\mathbf{H}_t)$ is the transverse electric(magnetic) field and $\mathbf{E}_z(\mathbf{H}_z)$ the longitudinal electric(magnetic) field. \mathbf{E}_t and \mathbf{H}_t can be expanded

$$\begin{cases} \mathbf{E}_t = \sum_{i=1}^2 \sum_{mn} V_{nm}^{(i)} \mathbf{e}_{nm}^{(i)}, \\ \mathbf{H}_t = \sum_{i=1}^2 \sum_{mn} I_{nm}^{(i)} \mathbf{h}_{nm}^{(i)}, \end{cases} \quad (15)$$

where $i = 1, 2$ represent electrical and magnetic mode of field. $V_{mn}^{(i)}$ and $I_{mn}^{(i)}$ are the profile function of the RF electric and magnetic field amplitudes, and $\mathbf{e}_{nm}^{(i)}$ and $\mathbf{h}_{nm}^{(i)}$ are orthogonal normalized wave function. They satisfy

$$\begin{cases} \iint_s \mathbf{e}_{nm}^{(i)} \cdot \mathbf{e}_{n'm'}^{(i')} ds = \delta(i - i') \delta(m - m') \delta(n - n'), \\ \iint_s \mathbf{h}_{nm}^{(i)} \cdot \mathbf{h}_{n'm'}^{(i')} ds = \delta(i - i') \delta(m - m') \delta(n - n'). \end{cases} \quad (16)$$

Using(14)~(16), the first-order transmission line equations are derived

$$\begin{cases} \frac{dV_{mn}^{(i)}}{dz} = -Z_{mn}^{(i)} \gamma_{mn}^{(i)} I_{nm}^{(i)} + \sum_{i'} \sum_{mn'} V_{mn'}^{(i')} Co_{(n',n)}^{(i',i)}, \\ \frac{dI_{mn}^{(i)}}{dz} = -\frac{\gamma_{mn}^{(i)}}{Z_{mn}^{(i)}} V_{nm}^{(i)} + \sum_{i'} \sum_{mn'} I_{mn'}^{(i')} Co_{(n',n)}^{(i',i)}, \end{cases} \quad (17)$$

where $Z_{mn}^{(i)}$ is the wave impedance, $Z_{mn}^{(1)} = \frac{\gamma_{mn}^{(1)}}{j\omega\epsilon}$, $Z_{mn}^{(2)} = \frac{j\omega\mu}{\gamma_{mn}^{(2)}}$, $Co_{(n',n)}^{(i',i)}$ the mode coupling coefficient and can be written as

$$Co_{(n',n)}^{(i',i)} = \iint_s \mathbf{e}_{mn'}^{(i')} \cdot \frac{\partial \mathbf{e}_{mn}^{(i)}}{\partial z} ds. \quad (18)$$

Equation (17) shows the distribution of profile function of the RF electric field of any mode along longitudinal axial z in a resonator. It can be applied not only to cylindrical resonators but also to coaxial resonator as well as coaxial outer corrugated resonator.

As known, all modes in a resonator must satisfy the boundary conditions at the input and output end of the resonator:

$$\begin{cases} \frac{dV_{mn}^{(i)}}{dz} - \gamma_{mn}^{(i)} V_{nm}^{(i)} = 0, & (z = 0), \\ \frac{dV_{mn}^{(i)}}{dz} + \gamma_{mn}^{(i)} V_{nm}^{(i)} = 0, & (z = L), \end{cases} \quad (19)$$

where $[\gamma_{mn}^{(i)}]^2 = [k_{mn}^{(i)}]^2 - \frac{\omega^2}{c^2}$, $\omega = \omega_0(1 + \frac{1}{2Q})$. By Equations (17) and (19), resonator frequency, quality factor and field profile distribution of the eigen-mode of the coaxial outer corrugated resonator can be calculated.

4. COUPLING COEFFICIENT

To research high frequency field in the coaxial outer corrugated resonator, by using (18), mode coupling coefficients is derived. By Green formula

$$\begin{cases} \iint_S (u \nabla_t^2 v - v \nabla_t^2 u) ds = \oint_c (u \nabla_t v - v \nabla_t u) \cdot \mathbf{i}_n dl, \\ \iint_S (\nabla_t v \nabla_t u + u \nabla_t^2 v) ds = \oint_c (u \nabla_t v) \cdot \mathbf{i}_n dl, \end{cases} \quad (20)$$

substituting $u = \frac{\partial \Phi_{ms}^{(i)}}{\partial z}$ and $v = \Phi_{mt}^{(j)}$ into (20) and using (6)~(9), (16) and (18), mode coupling coefficients are obtained

$$\left\{ \begin{aligned} Co_{(s,t)}^{(1,1)} &= \frac{\nu_{mt}^2}{\nu_{mt}^2 - \nu_{ms}^2} \frac{2}{\varepsilon_m G_{mt} G_{ms}} \left[\frac{J_m\left(\frac{\nu_{mt}}{C}\right) J_m\left(\frac{\nu_{ms}}{C}\right)}{J_m(\nu_{mt}) J_m(\nu_{ms})} \frac{1}{R_o} \frac{\partial R_o}{\partial z} - \frac{1}{R_i} \frac{\partial R_i}{\partial z} \right], \\ Co_{(s,t)}^{(2,2)} &= \frac{\chi_{ms} \chi_{mt}}{\chi_{ms}^2 - \chi_{mt}^2} \frac{2}{\varepsilon_m} \left\{ \frac{\frac{m^2}{\chi_{mt}^2} + \frac{w}{\chi_{mt}} + 1}{T_{mt} T_{ms}} \frac{1}{R_o} \frac{\partial R_o}{\partial z} - \frac{\frac{m^2 C^2}{\chi_{mt}^2} + 1}{K_{ms} K_{mt}} \frac{1}{R_i} \frac{\partial R_i}{\partial z} \right\}, \\ Co_{(s,s)}^{(1,1)} &= \frac{1}{\varepsilon_m G_{ms}^2} \left\{ \frac{1}{R_i} \frac{\partial R_i}{\partial z} - \frac{J_m^2\left(\frac{\nu_{ms}}{C}\right)}{J_m^2(\nu_{ms})} \frac{1}{R_o} \frac{\partial R_o}{\partial z} \right\}, \\ Co_{(t,t)}^{(2,2)} &= \frac{1}{\varepsilon_m} \frac{m^2}{\chi_{mt}^2} \left\{ \frac{C^2}{K_{mt}^2} \frac{1}{R_i} \frac{\partial R_i}{\partial z} - \frac{1}{T_{mt}^2} \frac{1}{R_o} \frac{\partial R_o}{\partial z} \right\}, \\ Co_{(s,t)}^{(1,2)} &= 0, \\ Co_{(s,t)}^{(2,1)} &= \frac{2m}{\varepsilon_m \chi_{ms} G_{mt}} \left\{ \frac{C}{K_{ms}} \frac{1}{R_i} \frac{\partial R_i}{\partial z} - \frac{1}{T_{ms}} \frac{J_m\left(\frac{\nu_{mt}}{C}\right)}{J_m(\nu_{mt})} \frac{1}{R_o} \frac{\partial R_o}{\partial z} \right\}, \end{aligned} \right. \quad (21)$$

where

$$T_{mn} = K_{mn} \frac{w Y_m(\chi_{mn}) + Y'_m(\chi_{mn})}{Y'_m\left(\frac{\chi_{mn}}{C}\right)}, \quad (22)$$

ε_m , G_{mn} and K_{mn} are determined by (10), (11), (12), respectively.

(21) is the mode coupling coefficient for the coaxial outer corrugated resonator, which shows a different mode relation in the resonator.

5. NUMERICAL RESULTS

From (4) and (21), it is found that the dispersion equation and coupling coefficient have relations with w which is determined by d , l and s . Hence, we research the effect of d , l , s as well as θ_i , θ_{o1} , θ_{o2} on the resonant frequency and quality factor. A coaxial outer corrugated resonator is designed in Fig. 2. Its normalized geometry parameters are shown in Table 1.

According to (17), (19) and (21), using numerical method, some results are found: resonant frequency is 170.08689 GHz, and Q -factor is 1856.19287; eigen-curves, mode coupling coefficients and field profiles

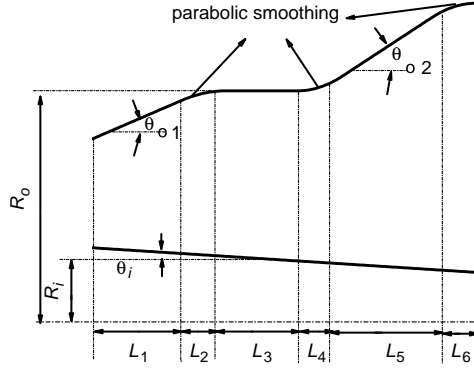


Figure 2. Longitudinal section.

Table 1. The normalized geometric parameter of coaxial outer corrugated resonator.

L_1	L_2	L_3	L_4	L_5	L_6	N
19	3.8	11.4	3.8	24.7	3.8	275
R_i	R_o	d	l	θ_i	θ_{o1}	θ_{o2}
7.29	28.8	0.57	0.42	1°	3°	2.5°

are obtained in Fig. 3. Fig. 3(a) shows that eigen-values of mode $TE_{34,17}$, $TE_{34,18}$ and $TE_{34,19}$ descend in the region $0 \leq z \leq 22.8$ and $34.2 \leq z \leq 66.5$, however, they don't almost change in the region $22.8 \leq z \leq 34.2$, which is caused by R_o keeping constant.

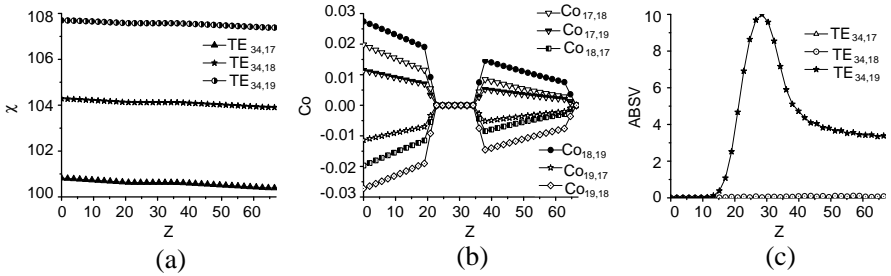


Figure 3. (a) Eigen-curve $\chi_{34,17}$, $\chi_{34,18}$ and $\chi_{34,19}$ versus z . (b) Mode coupling coefficient between $TE_{34,17}$, $TE_{34,18}$ and $TE_{34,19}$ versus z . (c) Field profiles for $TE_{34,17}$, $TE_{34,18}$ and $TE_{34,19}$ versus z .

Fig. 3(b) denotes that coupling coefficient between mode $TE_{34,17}$, $TE_{34,18}$ and $TE_{34,19}$ are symmetric to axis $Co = 0$ and they change greatly in the region parabolic segment $19 \leq z \leq 22.8$, $34.2 \leq z \leq 38$ and $62.7 \leq z \leq 66.5$, which imply that different mode keep energy exchange. Fig. 3(c) shows that mode $TE_{34,19}$ has an advantage over mode $TE_{34,17}$ and $TE_{34,18}$ in the resonator.

To study the effect of geometric parameter on frequency of high field and Q factor, calculation results are derived when d and l change, and the rest geometric parameters keep constant, respectively, which are shown in Table 2 and Table 3. Table 2 and Table 3 indicate that Q

Table 2. Resonant frequencies and diffractive quality factor of $TE_{34,19}$ versus the outer slot depth under the rest parameters keeping constant.

slot depth d	slot tooth width l	resonant frequency (GHz)	Q factor
0.53	0.42	169.82809	1816.49372
0.54	0.42	169.90176	1830.25465
0.55	0.42	169.96894	1841.12706
0.56	0.42	170.03042	1849.53652
0.57	0.42	170.08689	1856.19287
0.58	0.42	170.13898	1861.52392
0.59	0.42	170.18721	1867.68926
0.60	0.42	170.23206	1875.00779
0.61	0.42	170.27390	1881.32142
0.62	0.42	170.31309	1886.70753

Table 3. Resonant frequencies and diffractive quality factor of $TE_{34,19}$ versus the outer tooth width under the rest parameters keeping constant.

slot depth d	slot tooth width l	resonant frequency (GHz)	factor Q
0.57	0.38	169.95885	1837.82405
0.57	0.39	169.98986	1842.46612
0.57	0.40	170.02154	1847.10375
0.57	0.41	170.05389	1851.69527
0.57	0.42	170.08689	1856.19287
0.57	0.43	170.12055	1860.54354
0.57	0.44	170.15485	1864.69131
0.57	0.45	170.18976	1868.58086
0.57	0.46	170.22528	1872.78487
0.57	0.47	170.26140	1878.51213

value and frequency f rise slightly when d changes from 0.53 to 0.62, l from 0.38 to 0.47, and the rest parameters keep constant, respectively.

In addition, the effects of the slope angle θ_i of the inner conductor, and the asymptotic angle θ_{o1} and θ_{o2} of the outer conductor on resonant frequency and quality factor Q are also studied. Table 4 denotes that

Table 4. Resonant frequencies and diffractive quality factor of TE_{34,19} versus the slope angle of inner conductor under the rest parameters keeping constant.

θ_i	resonant frequency (GHz)	factor Q
0.0	170.08717	1841.959259
0.2	170.08714	1844.725721
0.4	170.08709	1847.501426
0.6	170.08704	1850.316211
0.8	170.08697	1853.201967
1.0	170.08689	1856.192876
1.2	170.08681	1859.325733
1.4	170.08670	1862.640374
1.6	170.08658	1866.180184
1.8	170.08645	1869.992719
2.0	170.08629	1874.130436

Table 5. Resonant frequencies and diffractive quality factor of TE_{34,19} versus the asymptotic angle θ_{o1} of outer conductor under the rest parameters keeping constant.

θ_{o1}	resonant frequency (GHz)	Q factor
2.0	170.08083	2025.533882
2.2	170.08233	1983.640430
2.4	170.08366	1946.567825
2.6	170.08485	1913.407038
2.8	170.08592	1883.461873
3.0	170.08689	1856.192875
3.2	170.08778	1831.176962
3.4	170.08859	1808.078251
3.6	170.08934	1786.626915
3.8	170.09003	1766.603738
4.0	170.09067	1748.770105

Q value rises and f decreases slightly when θ_i varies from 0° to 2° . Table 5 shows that Q value decreases greatly and f increases slightly when θ_{o1} varies from 2° to 4° . Table 6 displays that f rises slightly and Q value fluctuates when θ_{o1} varies from 2° to 4° .

Table 6. Resonant frequencies and diffractive quality factor of TE_{34,19} versus the asymptotic angle θ_{o2} of outer conductor under the rest parameters keeping constant.

θ_{o2}	resonator frequency (GHz)	Q factor
1.5	170.074790	1548.477564
1.7	170.080599	1570.930914
1.9	170.087995	1539.198703
2.1	170.088099	1750.381375
2.3	170.089364	1736.316631
2.5	170.086899	1856.192876
2.7	170.087512	1770.768354
2.9	170.086279	1815.727164
3.1	170.085420	1684.606696
3.3	170.089155	1737.057758
3.5	170.090137	1641.440053

Hence, results show that the field frequency and quality factor Q rise slightly when outer slot depth and tooth width increase, respectively. The field frequency almost keeps constant when asymptotic angle of outer conductor and slope angle of inner conductor rise, respectively. However, the quality factor Q rises slightly when the slop angle θ_i of inner conductor increases; factor Q decreases greatly when the first asymptotic angle θ_{o1} of conductor increases; factor Q fluctuates when the second asymptotic angle θ_{o2} of the outer conductor increases.

6. SUMMARY

In the paper, coaxial outer corrugated resonators are studied. By the surface impedance method, the resonator's dispersion equation is derived. Based on the transmission line and coupling wave theory, the resonator's transmission line equations and mode coupling coefficients are obtained. It is found in the results that outer slot depth and tooth width of the resonator slightly affect the field frequency and quality factor Q and that θ_i , θ_{o1} and θ_{o2} greatly affect Q value. But, they

almost do not affect the frequency. These results are beneficial to the design of gyrotron and the research on the interaction of beam-wave in high frequency and high power gyrotron.

ACKNOWLEDGMENT

This work is supported by the Scientific Research Foundation of Sichuan Provincial Department of Education under Grant No. 10ZC059.

REFERENCES

1. Grudiev, A., J. Y. Raguin, and K. Schunemann, "Numerical study of mode competition in coaxial cavity gyrotrons with corrugated insert," *Int. J. Infrared Millimeter Waves*, Vol. 24, 173–187, 2003.
2. Singh, K., P. K. Jain, and B. N. Basu, "Analysis of a corrugated coaxial waveguide resonator for mode rarefaction in a gyrotron," *IEEE Trans. Plasma Sci.*, Vol. 33, No. 3, 1024–1030, 2005.
3. Iatrou, C. T., "Mode selective properties of coaxial gyrotron resonators," *IEEE Trans. Plasma Sci.*, Vol. 24, No. 3, 596–605, 1996.
4. Iatrou, C. T., S. Kern, and A. B. Pavelyev, "Coaxial cavities with corrugated inner conductor for gyrotrons," *IEEE Trans. on Microwave Theory Tech.*, Vol. 44, No. 1, 56–64, 1996.
5. Dumbrajs, O. and G. I. Zaginaylov, "Ohmic losses in coaxial gyrotron cavities with corrugated insert," *IEEE Trans. Plasma Sci.*, Vol. 32, No. 3, 861–866, 2004.
6. Zaginaylov, G. I., N. N. Tkachuk, V. L. Shcherbinin, and K. Schuenemann, "Rigorous calculation of energy losses in cavity of ITER relevant coaxial gyrotron," *Proc. of 35th EuMW*, 1107–1110, 2005.
7. Zaginaylov, G. I. and I. V. Mitina, "Electromagnetic analysis of coaxial gyrotron cavity with the inner conductor having corrugations of an arbitrary shape," *Progress In Electromagnetics Research B*, Vol. 31, 339–356, 2011.
8. Ioannidis, Z. C., O. Dumbrajs, and I. G. Tigelis, "Linear and non-linear inserts for genuinely wide-band continuous frequency tunable coaxial gyrotron cavities," *Int. J. Infrared Millimeter Waves*, Vol. 29, No. 4, 416–423, 2008.
9. Piosczyk, B., A. Arnold, G. Dammertz, et al., "Coaxial cavity gyrotron-recent experimental results," *IEEE Trans. Plasma Sci.*, Vol. 30, No. 3, 819–827, 2002.

10. Flyagin, V. A. and G. S. Nusinovich, "Gyrotron oscillators," *Proceedings of the IEEE*, Vol. 76, 644–656, Oct. 1988.
11. Felch, K., H. Huey, and H. Jory, "Gyrotrons for ECH applications," *J. Fusion Energy*, Vol. 9, 59–75, 1990.
12. Makowski, M., "ECRF systems for ITER," *IEEE Trans. Plasma Sci.*, Vol. 24, 1023–1032, 1996.
13. Thumm, M., "MW gyrotron development for fusion plasma applications," *Plasma Physics and Controlled Fusion*, Vol. 45, No. 12A, 143–161, 2003.
14. Dammertz, G., S. Alberti, A. Arnold, et al., "High-power gyrotron development at Forschungszentrum Karlsruhe for fusion applications," *IEEE Trans. Plasma Sci.*, Vol. 34, No. 2, 173–186, 2006.
15. La Haye, R. J., et al., "Control of neoclassical tearing modes in DIII-D," *Phys. Plasmas*, Vol. 9, 2051–2051, 2002.
16. Dammertz, G., E. Borie, C. T. Iatrou, M. Kuntze, B. Pioscyk, and M. K. Thumm, "140-GHz gyrotron with multimegawatt output power," *IEEE Trans. Plasma Sci.*, Vol. 28, No. 3, 561–566, 2000.
17. Borie, E. and O. Dumbrajs, "Calculation of eigenmodes of tapered gyrotron resonators," *International Journal of Electron.*, Vol. 60, No. 2, 143–154, 1986.
18. Liu, R. and H. Li, "Study of eigenmodes of coaxial resonators using coupled-wave theory," *J. Infrared Milli. Terahertz Waves*, Vol. 31, 995–1003, 2010.